

AperTO - Archivio Istituzionale Open Access dell'Università di Torino

## **XAS and XES techniques shed light on the dark side of Ziegler-Natta catalysts: Active-site generation**

### **This is the author's manuscript**

*Original Citation:*

*Availability:*

This version is available <http://hdl.handle.net/2318/1530996> since 2016-09-12T17:54:58Z

*Published version:*

DOI:10.1002/cctc.201402989

*Terms of use:*

Open Access

Anyone can freely access the full text of works made available as "Open Access". Works made available under a Creative Commons license can be used according to the terms and conditions of said license. Use of all other works requires consent of the right holder (author or publisher) if not exempted from copyright protection by the applicable law.

(Article begins on next page)





# UNIVERSITÀ DEGLI STUDI DI TORINO

***This is an author version of the contribution published on:***

***[ChemCatChem 7 (9), pp. 1432-1437, (2015) DOI: 10.1002/cctc.201402989]***

***The definitive version is available at:***

***[<http://onlinelibrary.wiley.com/doi/10.1002/cctc.201402989/abstract>]***

# XAS and XES techniques try to shed light on the dark side of Ziegler-Natta catalysts: active sites generation

Elena Groppo,<sup>[a]</sup> Erik Gallo,<sup>[a,b]</sup> Kalaivani Seenivasan,<sup>[a]</sup> Kirill A. Lomachenko,<sup>[a,c]</sup> Anna Sommazzi,<sup>[d]</sup> Silvia Bordiga,<sup>[a]</sup> Pieter Glatzel,<sup>[b]</sup> Roelof van Silfhout,<sup>[e]</sup> Anton Kachatkou,<sup>[e]</sup> Wim Bras,<sup>[f]</sup> Carlo Lamberti<sup>[a,c]</sup>

**Abstract:** The local structure and the electronic properties of the active Ti sites in heterogeneous Ziegler-Natta catalysts, generated in situ by interacting the pre-catalyst with different Al-alkyl activators, are investigated by combining X-ray absorption and emission spectroscopy (XAS and vtc-XES), coupled with UV-Vis, FT-IR and DFT theoretical calculations. Irrespective of the activator used, the active system was found to be a highly dispersed TiCl<sub>3</sub>-like phase where the Ti sites are surrounded not only by bridged chlorine ligands (at the same bond distance of bulk TiCl<sub>3</sub>), but also by terminal chlorine ligands, at a much shorter distance. These results definitely set Ziegler-Natta catalysts in the category of complex nano-materials. Despite the observation that the investigated catalysts polymerize ethylene, at present cutting edge XAS and XES techniques do not offer yet univocal proofs for the presence of any alkyl chain attached to the Ti sites, as a consequence of the small fraction of the active sites.

Covering still increasing volumes of the polyolefin production sector (that is approaching 150 MTons/year),<sup>[1-6]</sup> heterogeneous Ziegler-Natta (ZN) catalysts are among the most productive and versatile catalytic systems in use in the chemical industry. Their versatility can be traced back to the complexity of their chemical composition. Actual generation of heterogeneous ZN catalysts comprise multiple components,<sup>[1-6]</sup> among which the fundamental ones are: i) the active phase, usually a transition metal halide of the 4<sup>th</sup> periodic table group; ii) a poorly crystalline MgCl<sub>2</sub>-based phase that increases the dispersion of the active

phase; iii) electron donor molecules, which influence the selectivity in the  $\alpha$ -olefins polymerization, and iv) the co-catalyst, usually an aluminum alkyl (such as AlR<sub>3</sub>, R = alkyl chain). The exact role of each component and their interconnection is far from being understood, and the development of these catalysts is still more driven by trial-and-error approaches than by a rational design.<sup>[7]</sup>

One of the important, but still unanswered, questions concerns the structure (at the molecular level) of the active sites in the catalyst obtained after interaction of the pre-catalyst with the Al-alkyl activator. Indeed, this step is usually performed directly inside the reactor in presence of the olefin monomer, so that the generation of the active sites is immediately followed by polymerization. According to the pioneering works of Cossee and Arlman,<sup>[8-10]</sup> the essential role of AlR<sub>3</sub> consists in the alkylation of the titanium ions where chlorine vacancies are available; although universally accepted, this statement relies entirely on quantum chemical principles and on the crystal chemistry of transition metal chloride structures; whereas direct experimental evidence of the structure of the active sites is still missing. Several reasons account for this lack of information, among which the most critical ones are the rapid deactivation (i.e. rearrangement of the Ti-R bond, which undergoes an easy  $\beta$ -elimination reaction) and the small fraction of the active sites,<sup>[11]</sup> along with the difficulty in handling the AlR<sub>3</sub> activator. All these problems contribute in rendering the active sites elusive to most experimental techniques.<sup>[12]</sup> As a matter of fact, the majority of experimental data on ZN catalysts refer to the pre-catalyst or, at most, to aged catalysts.

In the present work we focus our attention on a particular class of heterogeneous ZN catalysts, based on Ti and Mg chloride tetrahydrofuranates (thf: tetrahydrofuran), that have been patented long time ago for polyethylene production<sup>[13]</sup> and have been recently "re-discovered" for basic studies by means of multiple experimental methods.<sup>[14-18]</sup> The specific goal is to gain insights into the electronic properties and the local structure around the Ti active sites (in terms of number and type of ligands, and of coordination distances), and to provide direct evidence (if possible) of the presence of Ti-alkyl bond. To this end, we combined two synchrotron-based techniques that have the advantage to be element-selective: i) Ti K-edge X-ray Absorption Spectroscopy (XAS)<sup>[19,20]</sup> and ii) valence-to-core X-ray Emission Spectroscopy (vtc-XES).<sup>[21,22]</sup> The XAS and XES experiments were performed at the BM26A<sup>[23]</sup> and ID26 beamlines at the ESRF facility (Grenoble, France), respectively. Both measurements required the adoption of challenging experimental set-ups. In particular, to overcome the experimental difficulties due to beam drift and minute sample in-

- [a] Dr. E. Groppo, Dr. E. Gallo, Dr. K. Seenivasan, Kirill A. Lomachenko, Prof. S. Bordiga, Prof. C. Lamberti  
Department of Chemistry, INSTM and NIS Centre  
Università di Torino  
Via Quarello 15, 10135 Torino, Italy  
Fax: +39 011/6707855  
E-mail: [elena.groppo@unito.it](mailto:elena.groppo@unito.it)
- [b] Dr. E. Gallo, Dr. P. Glatzel  
European Synchrotron Radiation Facility,  
6 Rue Jules Horowitz, 38043 Grenoble, France
- [c] Kirill A. Lomachenko, Prof. C. Lamberti  
Southern Federal University  
Zorge Street 5, 344090 Rostov-on-Don, Russia
- [d] Dr. A. Sommazzi  
Versalis – Novara Research Center, Istituto Eni Donegani  
Via Fauser, 4 - 28100 Novara, Italy
- [e] Dr. Roelof van Silfhout, Anton Kachatkou  
The University of Manchester  
Sackville Street, Manchester M13 9PL, United Kingdom
- [f] Dr. Wim Bras  
Netherlands Organization for Scientific Research  
Dubble@ ESRF, Grenoble, France

Supporting information for this article is given via a link at the end of the document.

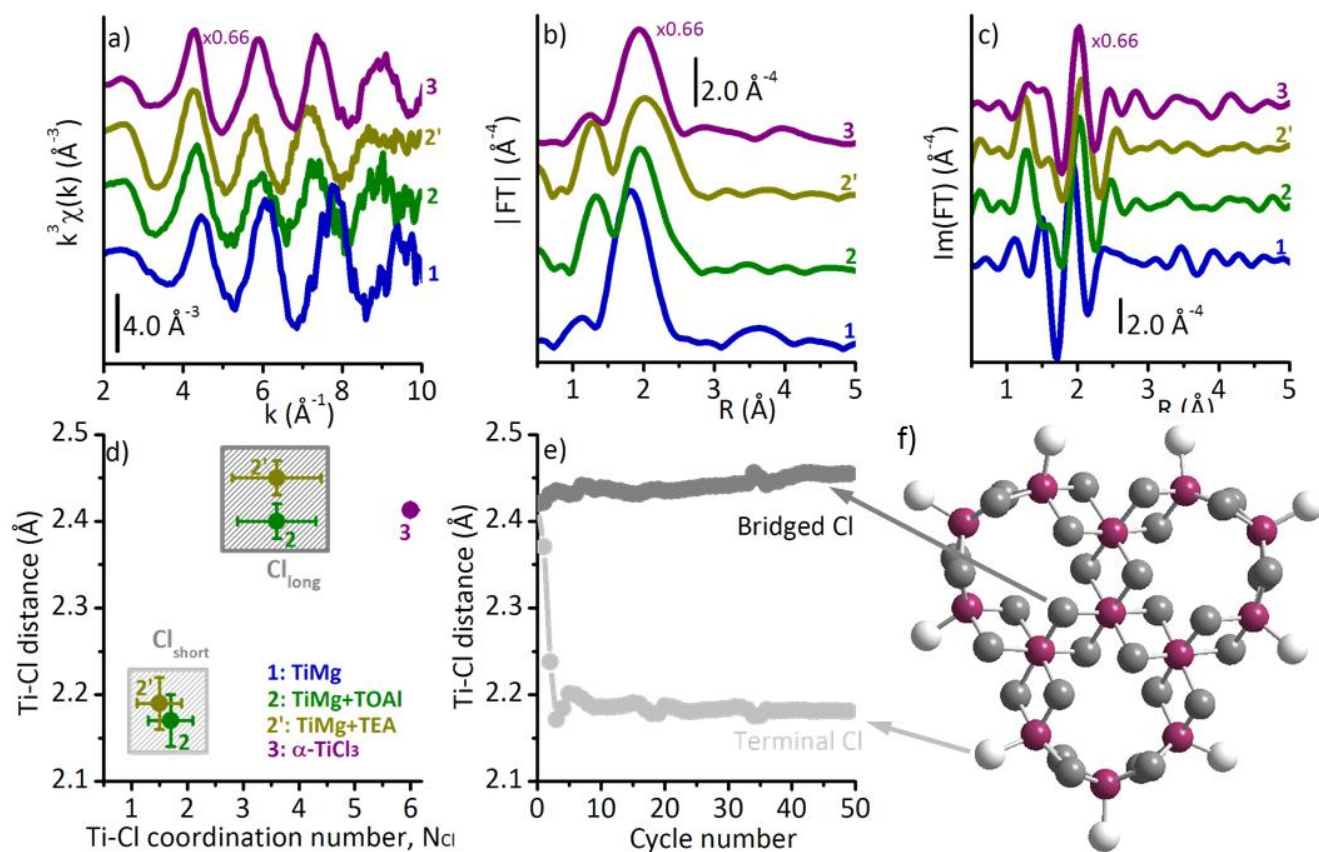


**Figure 1.** Parts a) – c):  $k^3$ -weighted  $\chi(k)$  functions and corresponding Fourier Transforms (in both modulus and imaginary parts) of the TiMg pre-catalyst (1) and of the same sample after interaction with TOAI (2) and TEA (2'). Also the spectrum of violet  $\text{TiCl}_3$  (3), multiplied by a factor of 0.66, is shown for comparison. The spectra were vertically translated for clarity. Part d): summary of the fitted Ti-Cl distances (in Å) and of the corresponding coordination numbers  $N(\text{Cl})$ , as resulting from the data analysis of the EXAFS data shown in parts a)-c). Grey boxes highlight the contributions of two different chlorine ligands, at shorter ( $\text{Cl}_{\text{short}}$ ) and longer ( $\text{Cl}_{\text{long}}$ ) bond distances, respectively. Part e): Evolution of the Ti-Cl bond distances for central and terminal titanium atoms during the geometry optimization, carried out at DFT level on the cluster shown in Part f). Bridged chlorine, terminal chlorine and titanium atoms are shown in dark grey, light grey and violet, respectively. Arrows indicate the bonds whose distances were being monitored.

homogeneities intrinsic to XAS experiments on heterogeneous catalysts at these low X-ray energies, it was necessary to develop a feedback mechanism on the X-ray optics of BM26.<sup>[24]</sup> Moreover, because of the high photon flux adopted during vtc-XES measurements (more than  $10^{12}$  photons per second), the samples were found to suffer of radiation damage on a fast time scale ( $\sim 10$  s). To circumvent this problem, each point of the vtc-XES spectrum was collected on a different sample spot irradiated for 2 seconds, and the intensity was normalized to the total fluorescence yields signal recorded with a solid state detector. The micrometric size of the beam allowed us to have sufficient fresh points on the sample (1.3 cm diameter pellet) to collect a full vtc-XES spectrum. Manipulation and measurements of all the samples were performed under strictly inert conditions. Further details on the experimental set-ups are given in the Supporting Information. The XAS-XES data were complemented with Diffuse Reflectance (DR) UV-Vis and FT-IR results, as well as with DFT theoretical calculations.

The pre-catalyst (hereafter TiMg) was obtained by reacting together the  $\text{MgCl}_2(\text{thf})_{1.5}$  and  $\text{TiCl}_4(\text{thf})_2$  precursors in thf, as reported in the Experimental Section.<sup>[14]</sup> For Mg/Ti molar ratio equal to 2, a crystalline bi-metallic adduct is formed:  $\text{TiCl}_4(\text{thf})_2$

removes  $\text{Cl}^-$  from  $\text{MgCl}_2(\text{thf})_{1.5}$  to form the  $[\text{TiCl}_5(\text{thf})]^-$  anion; the counter-cation is a dimeric Mg-chloride tetrahydrofuranate.<sup>[14,25,26]</sup> The local structure around the Ti atoms is elucidated by the EXAFS data (Figure 1). The FT of the  $k^3$ -weighted  $\chi(k)$  function (Figure 1a,b) is dominated by a first shell peak centered around  $1.8 \text{ Å}$  (not phase-corrected), which is the result of the sum of the 6 single-scattering contributions deriving from the first shell ligands (*i.e.* 1 O belonging to the thf moiety at  $2.19 \pm 0.08 \text{ Å}$ , 1 Cl at  $2.28 \pm 0.08 \text{ Å}$  and 4 Cl at  $2.34 \pm 0.08 \text{ Å}$ , see Section S3 of the Supporting Information for a detailed analysis). In the resulting TiMg bimetallic salt the Ti sites have a +4 oxidation state and show a 6-fold coordination,<sup>[12]</sup> as monitored by DR UV-Vis, XANES and  $K\beta$ -XES spectroscopy (Figure 2). In particular: i) the intense absorption around  $25000 \text{ cm}^{-1}$  in the DR UV-Vis spectrum (Figure 2a) is assigned to fully allowed  $\text{Cl}(p) \rightarrow \text{Ti}(d)$  ligand-to-metal charge-transfer transitions, where the excited electron is associated with one of the nearest Cl anion and the transferred electron goes into a 3d orbital of the  $\text{Ti}^{4+}$  ion;<sup>[14,27-30]</sup> ii) the weak pre-edge peak at  $4970.6 \text{ eV}$  (shoulder at  $4968.3 \text{ eV}$ ) in the XANES spectrum (Figure 2b), that precedes the absorption edge at  $4979 \text{ eV}$ , is due to  $1s \rightarrow pd$  transitions;<sup>[14,31-34]</sup> iii) the two

$K\beta''$  lines present in the vtc-XES spectrum (Figure 2c) at 4947 and 4953 eV are due to transitions mainly involving molecular orbitals having primarily O(2s) and Cl(3s) character, and thus identify the presence of oxygen and chlorine ligands in the first coordination sphere of the Ti sites.<sup>[35-37]</sup>

The catalysts were obtained from the above mentioned pre-catalyst upon interaction with the  $\text{AlR}_3$  activator. In order to limit catalyst deactivation, excess of  $\text{AlR}_3$  was used, and this step was performed immediately before the spectroscopic measurements. In some cases triethylaluminum (TEA, Aldrich, pure) was used, in others trioctylaluminum (TOAI, Aldrich, 25% diluted in heptane). As a proof that the so obtained catalyst is active in ethylene polymerization, Figure 3 shows the FT-IR spectrum (collected in Attenuated Total Reflection mode) of  $\text{TiMg}+\text{TEA}$  after polymerization of  $\text{C}_2\text{D}_4$  at room temperature. Deuterated ethylene was used to clearly detect the presence of polyethylene by IR spectroscopy, without interfering with the vibrational modes of the  $\text{AlR}_3$  activator. The spectrum, dominated by the IR absorption bands of TEA and residual thf, clearly shows the characteristic  $\nu(\text{CD}_2)$  bands of deuterated polyethylene at 2193 and 2088  $\text{cm}^{-1}$  (inset in Figure 3).

The effects of Al-alkyls on the pre-catalyst are remarkable, and involve both the local structure, as revealed by EXAFS (Figure 1) and the electronic properties, as detected by DR UV-Vis, XANES and vtc-XES (Figure 2). EXAFS spectra of the two catalysts obtained after interaction of  $\text{TiMg}$  with TOAI and TEA (Figure 1a) are substantially different from that of  $\text{TiMg}$ . This observation provides an evidence that  $\text{AlR}_3$  cause a drastic structural change in the pre-catalyst. This is valid not only for the  $\text{MgCl}_2$  phase, as previously demonstrated by XRPD,<sup>[14,25]</sup> but also for all the Ti species, whose structure can not be elucidated by XRPD because of the absence of a long-range order. The effect is the same irrespective of the activator used. Moreover, the spectra of the catalysts are both very similar to that of violet  $\text{TiCl}_3$ , although 1/3 less intense, suggesting that the local structure of the new Ti phase is analogous to that of  $\text{TiCl}_3$ . A closer inspection of the FT of the  $k^3$ -weighted  $\chi(k)$  functions (Figure 1b,c) reveals that the first shell signal is split in two

components, well evident as a beat at 1.6 Å in the  $\text{Imm}(\text{FT})$ . The additional contribution at low R values might be due to a carbon atom belonging to an alkyl chain, in agreement with the postulated Cossee-Arlman mechanism.<sup>[8-10]</sup> Unfortunately, any attempt to fit the experimental spectrum with a Ti-C contribution yielded unsatisfactory results (see Section S4 of the Supporting Information). Instead, good results were obtained by considering that two types of chlorine ligands, at shorter ( $\text{Ti-Cl}_{\text{short}}$ ) and longer ( $\text{Ti-Cl}_{\text{long}}$ ) distance, exist and contribute to define the coordination sphere around the Ti sites.

A summary of the fitted Ti-Cl distances and of the corresponding coordination numbers ( $N_{\text{Cl}}$ ) is shown in Figure 1d. Coordination numbers of about 5.3 for  $\text{TiMg}+\text{TOAI}$  and 5.1 for  $\text{TiMg}+\text{TEA}$  were obtained, to be compared with 6.0 for violet  $\text{TiCl}_3$ . Coordination numbers smaller than in the reference indicate that a fraction of the Ti atoms (those at the surface) do have at least one vacancy in their coordination sphere (i.e. a fraction of Ti atoms have less than six chlorine ligands). Within the experimental error, the  $\text{Ti-Cl}_{\text{long}}$  distances were found to vary in the 2.40 – 2.50 Å range, and are slightly shorter for the catalyst prepared with TOAI than with TEA (appreciable also in the rough FT data, Figure 1a,b). It is worth noticing that the characteristic Ti-Cl distance for bridged chlorine ligands in violet bulk  $\text{TiCl}_3$  is 2.42 Å, whereas in bulk  $\text{TiCl}_2$  it increases to 2.50 Å. Therefore, the longer  $\text{Ti-Cl}_{\text{long}}$  distance found for  $\text{TiMg}+\text{TEA}$  catalysts suggests the presence of  $\text{Ti}^{2+}$  species, in agreement with the XANES and DR UV-Vis results (see below).

Additional chlorine ligands at a distance shorter ( $\text{Ti-Cl}_{\text{short}}$ ) than that characteristic of bridged chlorine ligands in violet  $\text{TiCl}_3$  characterize the Ti coordination sphere in the two catalysts. Similar results were previously reported by other authors for similar systems ( $\text{TiCl}_3/\text{MgCl}_2$ <sup>[33]</sup> and  $\text{TiCl}_4/\text{MgCl}_2+\text{TEA}$ <sup>[38]</sup>) although with unlikely small coordination numbers. In these works,<sup>[33,38]</sup> the short Ti-Cl distances were interpreted in terms of close interaction of the highly dispersed  $\text{TiCl}_3$  phase with the  $\text{MgCl}_2$  phase, which occurs through a bridged chlorine species. However, we noticed that Ti-Cl distances around 2.20 Å are characteristic of terminal chlorine ligands.

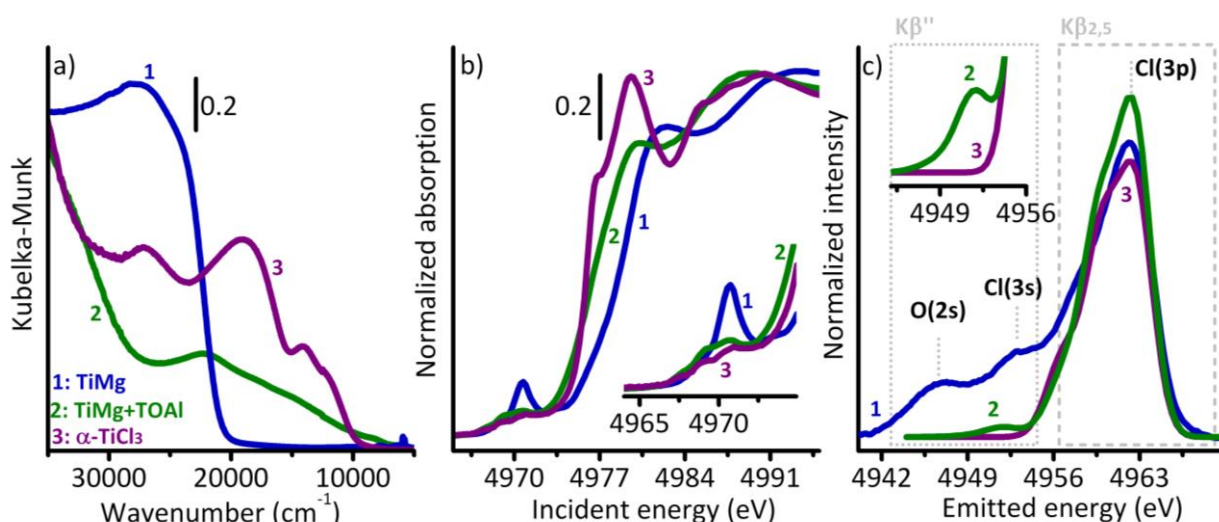


**Figure 2.** Diffuse Reflectance UV-Vis (in Kubelka-Munk units, part a), normalized Ti K-edge XANES (part b) and normalized vtc-XES (part c) spectra of the  $\text{TiMg}$  pre-catalyst (1) and of the catalysts obtained after interaction of  $\text{TiMg}$  with excess of TOAI (2). The spectra of violet  $\text{TiCl}_3$  are also shown for comparison (3). Inset in part b) shows a magnification of the pre-edge region in the XANES spectra. Inset in part c) shows a magnification of spectra 2 and 3 in the 4950-4956 eV region. The main peaks in the vtc-XES spectra are also assigned. The  $K\beta''$  and  $K\beta_{2,5}$  regions are indicated with grey boxes.



On these basis, we carried out a geometry optimization at DFT level (Figure 1e) of a  $\text{TiCl}_3$  nano-cluster containing 13 Ti and 39 Cl atoms (Figure 1f); the cluster was cut from the  $\alpha\text{-TiCl}_3$  bulk structure with R-3 symmetry reported by Troyanov et al.<sup>[39]</sup>  $D_3$  symmetry for the cluster was enforced, mimicking the one of the bulk material. One chlorine ligand was removed for each Ti atom at the border, in order to maintain the  $\text{TiCl}_3$  stoichiometry and to simulate the presence of coordination vacancies. No other restrictions were imposed. In the initial model all the Ti-Cl distances were equal to 2.42 Å. However, in course of optimization the Ti-Cl distances evolved differently for bridged and terminal chlorine ligands (Figure 1e). Chlorine ligands bonded to the central (bulk-like) Ti atom were not significantly shifted compared to the initial positions; the resulting Ti-Cl bond length was 2.45 Å. On the contrary, for terminal chlorine ligands the Ti-Cl distances were significantly contracted compared to the bulk ones; optimization yielded the values of  $2.20 \pm 0.01$  Å depending on the terminal Ti site. It is worth noticing that virtually the same results were obtained for a cluster fully terminated with chlorine ligands. Hence, the Ti-Cl distances do not seem to be affected by the presence of a vacancy around the terminal titanium sites. However, the simple cluster shown in Figure 1f does not have the ambition to represent the active  $\text{TiCl}_x$  phase in the investigated catalyst. For example, it does not take into account the presence of the  $\text{MgCl}_2$  phase that is surely involved in the definition of the active phase. In this respect, it must be noticed that Cl ligands bridged to one Mg and one Ti instead of two Ti atoms are expected to have very similar Ti-Cl distances. Nevertheless, this simple cluster allows to interpret the EXAFS data. In particular, the following statements can be safely made: 1) the  $\text{AlR}_3$  activators transform the molecularly well defined  $\text{TiMg}$  precursor into a  $\text{TiCl}_x$  phase having a local structure very similar to that of violet  $\text{TiCl}_3$ , but a much larger fraction of terminal chlorine ligands, as a consequence of reduced dimensions; 2) the terminal Cl ligands are characterized by a much shorter Ti-Cl distance; and 3) at least a fraction of the Ti sites do have a coordination vacancy.

Coming to the electronic properties, in the DR UV-Vis spectra (Figure 2a and Figure S5a), a broad absorption appears in the visible region, which is typical of d-d transition for  $\text{Ti}^{3+}$  species in a 6-fold geometry.<sup>[12]</sup> Simultaneously, the intense absorption around  $25000\text{ cm}^{-1}$  shifts upward, as expected for a decrease in the Ti oxidation state. In the XANES spectra, the edge shifts to lower energy (Figure 2b and Figure S5b), suggesting that the Ti oxidation state is less than +4.<sup>[12]</sup> The pre-edge peak becomes less intense and structured into three bands at 4967, 4969, and 4971 eV (inset in Figure 2b). Finally, the vtc-XES spectrum of the catalyst (Figure 2c) does not show anymore the  $\text{K}\beta''$  lines characteristic of oxygen and chlorine ligands. Taken all together, these data provide an evidence that  $\text{AlR}_3$  reduce  $\text{Ti}^{4+}$  sites (mainly to  $\text{Ti}^{3+}$  for TOAI, and perhaps to a mixture of  $\text{Ti}^{3+}$  and  $\text{Ti}^{2+}$  for TEA), in agreement with literature results.<sup>[11]</sup> As for the EXAFS spectra, also the DR UV-Vis, XANES and vtc-XES spectra of the catalysts have strong similarities with the spectra of violet  $\text{TiCl}_3$  (spectra **3** in Figure 2), with some differences that are discussed in the following.

1) In the UV-Vis spectrum of the catalysts (Figure 1a and Figure S5a), the intense band higher than  $30000\text{ cm}^{-1}$  having a pure ligand-to-metal charge-transfer character, is perfectly overlapped to that of  $\text{TiCl}_3$ . On the contrary, the spectrum of the catalyst differs from that of  $\text{TiCl}_3$  in the visible range, where the absorption bands are less intense and broader. In this respect, it should be noticed that for  $\text{TiCl}_3$  the

assignment of the absorption bands in the  $12500\text{-}14000\text{ cm}^{-1}$  region (Jahn-Teller split d-d transitions of  $\text{Ti}^{3+}$  sites in a distorted 6-fold geometry) and higher than  $30000\text{ cm}^{-1}$  (fully allowed charge transfer p-d transitions) is firmly established;<sup>[30,40,41]</sup> whereas the nature of the couple of bands at around  $19000$  and  $27000\text{ cm}^{-1}$ , having an intensity intermediate between that of localized d-d transitions and that of charge-transfer transitions, was a matter of discussion in the specialized literature. Absorption bands in this energy regions are characteristic of many  $3d^1$  and  $3d^2$  transition metal-halides, and often overlap to produce relatively unstructured absorption responsible for a prevalence of black materials. The most common interpretation is that they are due to inter-site hopping transitions of the type  $2(3d^1) \rightarrow 3d^0 + 3d^2$ , involving couples of Ti sites bridged by chlorine ligands.<sup>[40,41]</sup> The much lower intensity of these bands in the UV-Vis spectrum of the catalyst might be an indication that they are mainly due to localized (intra-site) more than inter-site d-d transitions. This implies that, although bridged by chlorine ligands (as revealed by the charge-transfer band higher than  $30000\text{ cm}^{-1}$ ), the reduced Ti sites in the catalyst do not “communicate” each others. On the other hand, the broadness of the bands in the visible region reflects a larger heterogeneity of sites. Both conclusions (more localized transitions and heterogeneity) are in agreement with the hypothesis of a  $\text{TiCl}_x$  phase having reduced dimension.

2) In the XANES spectrum of the catalyst (Figure 2b and Figure S5b), the pre-edge features (which are due to localized transitions) are well overlapped to those of  $\text{TiCl}_3$ . On the contrary, the XANES spectrum of  $\text{TiCl}_3$  has a much more structured edge than that of the catalyst. In particular, a sharp feature is observed at 4980 eV (having a shoulder at 4977 eV), which was assigned to allowed  $\text{Ti}(1s) \rightarrow \text{Cl}(4p)$  transitions, enhanced by the multiple scattering contributions characteristic of well crystalline materials.<sup>[32,33,42]</sup> These features are absent in the XANES spectrum of the catalyst, suggesting that the multiple scattering contributions are limited. This observation is again in favor of a low-dimensional  $\text{TiCl}_x$  phase.

3) Finally, the vtc-XES spectrum of the catalyst and of violet  $\text{TiCl}_3$  show very similar  $\text{K}\beta_{2,5}$  lines (Figure 1c), which are due to transitions involving molecular orbitals having mainly a ligand p character.<sup>[43,44]</sup> Hence, the new  $\text{TiCl}_x$  phase formed in the catalyst should have the same valence orbitals of violet  $\text{TiCl}_3$ . On the contrary, a weak peak around 4952 eV is observed in the vtc-XES spectrum of the catalyst (inset in Figure 1c), which is not present in that of  $\text{TiCl}_3$ . In principle, transitions involving  $\text{Cl}(3s)$  molecular orbitals could contribute in this energy region (as indicated by the label for the  $\text{TiMg}$  pre-catalyst), provided that they also have a Ti p contribution.<sup>[35,36,45]</sup> Also C ligands having  $\text{sp}^3$  hybridization can contribute in the same energy region. As an example, the vtc-XES spectrum of  $\text{TiC}$  (Figure S6) shows a prominent band at 4954 eV, which identifies the  $\text{sp}^3$  hybridized carbon ligands. Hence, the weak band at 4952 eV observed in the vtc-XES spectrum of the catalyst might identify both chlorine and carbon ligands. We tried to discriminate between the two possibilities by DFT theoretical calculations conducted on the same  $\text{TiCl}_3$  nano-cluster adopted to validate the EXAFS data analysis (Figure 1f). However, simulation of the XES of  $\text{TiCl}_3$  appeared to be very challenging, in line with the results reported in the study of Sementa et al.,<sup>[46]</sup> and no

decisive conclusions could be drawn from them. Therefore, at the present stage, we are not able to univocally assign the weak band at 4952 eV observed in the vtc-XES spectrum of TiMg treated in excess of TOAI.

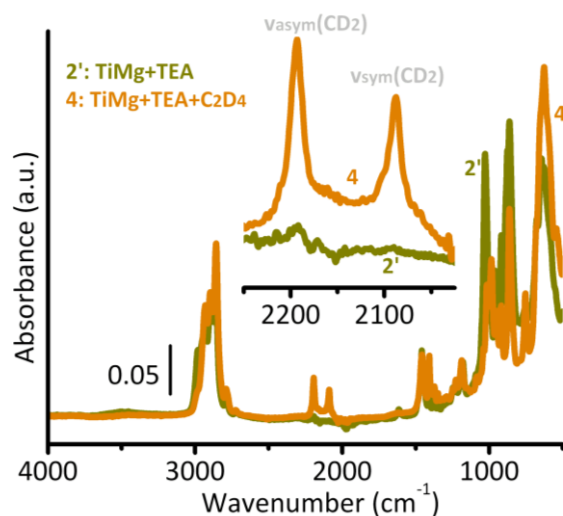


**Figure 3.** IR spectra, collected in ATR mode, of the TiMg+TEA catalyst before and after polymerization of  $C_2D_4$ . The inset shows a magnification of the  $\nu(CD_2)$  absorption bands.

In summary, the whole set of experimental and theoretical data discussed above give a contribution to the understanding of the role of aluminum alkyls in Ziegler-Natta catalysis. It was found that  $AlR_3$  activators reduce the  $Ti^{4+}$  sites originally present in the pre-catalyst, mainly to  $Ti^{3+}$  for TOAI, and probably to a mixture of  $Ti^{3+}$  and  $Ti^{2+}$  for TEA. The well-defined molecular structure of the TiMg pre-catalyst is completely destroyed by the activators, and a new highly dispersed  $TiCl_3$ -like phase is formed, in which the Ti sites are quite heterogeneous. Indeed, as a consequence of the limited particle size, the Ti sites are surrounded not only by bridged chlorine ligands (at the same bond distance of bulk  $TiCl_3$ ), but also by terminal chlorine ligands, at a much shorter distance. Moreover, a consistent fraction of the Ti sites contain a vacancy in the coordination sphere. The high dispersion of the active  $TiCl_3$ -like phase is testified by the observation that electronic transitions involving d electrons are more localized than for bulk  $TiCl_3$ . Despite the observation that the investigated catalysts polymerize ethylene, at present XAS and XES techniques do not offer univocal proofs for the presence of any alkyl chain (i.e. carbon ligand) attached to the Ti sites. This might be an indication that the number of Ti carrying the alkyl chain (i.e. the active sites in ethylene polymerization) is too small a fraction of the total Ti sites, and thus below the detection sensitivity of the adopted techniques. It must be noticed that even though the active Ti-alkyl sites were not identified, it was unambiguously experimentally observed that the active phase is originated from an extensive reconstruction of a well-defined TiMg pre-catalyst, and it is composed of  $TiCl_3$ -like nano-clusters (terminating with chlorine ligands having Ti-Cl bond distances much shorter than in the bulk). This finding has potentially many implications also for the more common Ziegler-Natta catalysts obtained from activation of the much less defined  $MgCl_2/TiCl_4$  pre-catalysts, where an even larger  $TiCl_x$  dispersion could be predicted. Hence, these results definitely set

Ziegler-Natta catalysts in the category of complex nano-materials, which is not yet completely recognized in the specialized literature. In this respect, any attempt to optimize these systems should start from the awareness that they need to be treated with adequate experimental and theoretical tools. Finally, it should be noticed that the problems encountered in this work are common to most of the heterogeneous catalysts; hence, the strategies here followed can offer some hints for the investigation of other catalytic systems.

## Experimental Section

The TiMg pre-catalyst was synthesized by dissolving separately  $TiCl_4(thf)_2$  and  $MgCl_2(thf)_{1.5}$  precursors into thf solvent, mixing both solutions ( $Mg : Ti = 2 : 1$ ) and leaving under stirring for 3 hours at room temperature. The solid product was recovered by evaporation of the solvent, washed with pentane dry and dried in vacuo. The yellow solid product obtained gave the following elemental analysis: Ti 5.9%; Mg 6.4%; Cl 32.4%.<sup>[14]</sup> The catalysts were obtained from the above mentioned pre-catalyst upon interaction with the  $AlR_3$  activator, as discussed in the text.

Ti K-edge XAS and vtc-XES spectra were collected at the BM26A (DUBBLE) and ID26 beamlines at the European Synchrotron Radiation Facility (ESRF, Grenoble, F), respectively. For both XAS and vtc-XES experiments, the samples were measured in the form of self-supporting pellets after mixing the powder with paraffin (transparent to X-ray), inside a home-made quartz cell equipped with two kapton windows. All the samples were manipulated in controlled atmosphere, inside an argon-filled glove-box. Argon was removed from the cell before the measurement, because it absorbs a high fraction of the incoming beam at the low energy of Ti K-edge. Further experimental details are given in the Supporting Information.

UV-Vis-NIR spectra were collected in diffuse reflectance mode on a Cary5000 Varian spectrophotometer. All the samples were measured in powdered form (diluted in Teflon) inside a cell having an optical window (suprasil quartz) and allowing one to perform measurements in controlled atmosphere. IR spectra were collected on a Bruker Alpha instrument, equipped with an Attenuated Total Reflection (ATR) accessory (diamond crystal), and placed inside the glove-box. The spectra were collected in the 4000-500  $cm^{-1}$  wavenumber region, at a resolution of 2  $cm^{-1}$ .

DFT calculations were carried out using ADF2013 code.<sup>[47,48]</sup> PBE exchange-correlation functional<sup>[49]</sup> combined with D3 Grimme dispersion correction<sup>[50]</sup> was used. Slater type basis sets were chosen for all atoms: TZ2P for chlorine and TZ2P+ with additional d orbitals for titanium.<sup>[51]</sup> Relativistic effects were dealt with employing ZORA approach.<sup>[52]</sup> Frozen core approximation was used, thus neglecting the changes occurring to core orbitals (up to 2p for both Ti and Cl) upon the formation of chemical bonds. Convergence criteria were set to 0.001 Hartree for energy, 0.001 Hartree/Å for gradients, and 0.01 Å for bond distances.

## Acknowledgements

Prof. A. Zecchina is gratefully acknowledged for his constant support, everyday encouragement and indispensable suggestions. We thank H. Müller (Chemical Lab at ESRF) for giving us access to the always perfect glove-box during the experiments at ESRF. This work was supported by "Progetti di Ricerca di Ateneo-Compagnia di San Paolo-2011- Linea 1", ORTO11RRT5 project. C.L. and K. A. L. thank the Mega-grant of the Russian Federation Government to support scientific research at Southern Federal University, No.14.Y26.31.0001.



**Keywords:** Ziegler-Natta catalysts • EXAFS • X-ray emission spectroscopy • surface active sites • in situ characterization

- [1] E. Albizzati, U. Giannini, G. Collina, L. Noristi, L. Resconi, *Catalysts and polymerizations*, in: Polypropylene Handbook; Moore, E. P. J., Ed.; Hanser-Gardner Publications: Cincinnati, OH, **1996**; Vol. Chapter 2.
- [2] R. Mulhaupt, *Macromol. Chem. Phys.* **2003**, *204*, 289–327.
- [3] L. L. Böhm, *Angew. Chem. -Int. Edit.* **2003**, *42*, 5010–5030.
- [4] G. Wilke, *Angew. Chem. -Int. Edit.* **2003**, *42*, 5000–5008.
- [5] P. Corradini, G. Guerra, L. Cavallo, *Acc. Chem. Res.* **2004**, *37*, 231–241.
- [6] V. Busico, *MRS Bulletin* **2013**, *38*, 224–228.
- [7] V. Busico, *Dalton Trans.* **2009**, 8794–8802.
- [8] P. Cossee, *J. Catal.* **1964**, *3*, 80–88.
- [9] E. J. Arlman, *J. Catal.* **1964**, *3*, 89–98.
- [10] E. J. Arlman, P. Cossee, *J. Catal.* **1964**, *3*, 99–104.
- [11] Y. V. Kissin, *Alkene Polymerization Reactions with Transition Metal Catalysts*; Elsevier, **2008**; Vol. 173.
- [12] E. Groppo, K. Seenivasan, C. Barzan, *Catal. Sci. Technol.* **2013**, *3*, 858–878.
- [13] U. Giannini, E. Albizzati, S. Parodi, F. Pirinoli, **1978**, US Patent, 4,124,532.
- [14] K. Seenivasan, A. Sommazzi, F. Bonino, S. Bordiga, E. Groppo, *Chem. Eur. J* **2011**, *17*, 8648–8656.
- [15] E. Grau, A. Lesage, S. Norsic, C. Copéret, V. Monteil, P. Sautet, *ACS Catal.* **2013**, *3*, 52–56.
- [16] W. Phiwklang, B. Jongsomjit, P. Praserttham, *J. Appl. Polym. Sci.* **2013**, *130*, 1588–1594.
- [17] S. Ntais, A. Siokou, *Surf. Sci.* **2006**, *600*, 4216–4220.
- [18] S. Ntais, V. Dracopoulos, A. Siokou, *J. Mol. Catal. A-Chem.* **2004**, *220*, 199–205.
- [19] S. Bordiga, E. Groppo, G. Agostini, J. A. Van Bokhoven, C. Lamberti, *Chem. Rev.* **2013**, *113*, 1736–1850.
- [20] L. Mino, G. Agostini, E. Borfecchia, D. Gianolio, A. Piovano, E. Gallo, C. Lamberti, *J. Phys. D-Appl. Phys.* **2013**, *46*.
- [21] P. Glatzel, T.-C. Weng, K. Kvashnina, J. Swarbrick, M. Sikora, E. Gallo, N. Smolentsev, R. A. Mori, *J. Electron Spectrosc. Relat. Phenom.* **2013**, *188*, 17–25.
- [22] C. Garino, E. Borfecchia, R. Gobetto, J. A. van Bokhoven, C. Lamberti, *Coord. Chem. Rev.* **2014**, *277–278*, 130–186.
- [23] S. Nikitenko, A. M. Beale, A. M. J. van der Eerden, S. D. M. Jacques, O. Leynaud, M. G. O'Brien, D. Detollenaere, R. Kaptein, B. M. Weckhuysen, W. Bras, *J. Synchrotr. Radiat.* **2008**, *15*, 632–640.
- [24] R. van Silfhout, A. Kachatkou, E. Groppo, C. Lamberti, W. Bras, *J. Synchrotron Radiat.* **2014**, *21*, 401–408.
- [25] I. Kim, M. C. Chung, H. K. Choi, J. H. Kim, S. I. Woo, *Stud. Surf. Sci. Catal.* **1990**, *56*, 323–343.
- [26] P. Sobota, *Chem.-Eur. J.* **2003**, *9*, 4854–4860.
- [27] C. K. Jorgensen, *Halogen Chemistry*; Academic Press: New York, **1967**; Vol. 1.
- [28] C. K. Jorgensen, *Progr. Inorg. Chem.* **1970**, *12*, 101–157.
- [29] R. J. H. Clark, D. Lewis, D. J. Machin, R. S. Nyholm, *J. Chem. Soc.* **1963**, 379–387.
- [30] R. J. H. Clark, *J. Chem. Soc.* **1964**, 417–425.
- [31] G. R. Shulman, Y. Yafet, P. Eisenberger, W. E. Blumberg, *Proc. Natl. Acad. Sci.* **1976**, *73*, 1384–1388.
- [32] G. Vlaic, J. C. J. Bart, W. Cavigliolo, A. Michalowicz, in: EXAFS and Near Edge Structure; Bianconi, A.; Incoccia, L.; Stipcich, S., Ed.; Springer: Berlin, **1983**, p. 307–309.
- [33] T. Usami, S. Takayama, M. Yokoyama, *J. Polym. Sci.* **1985**, *23*, 427–432.
- [34] F. Farges, G. E. Brown Jr, J. J. Rehr, *Phys. Rev. B* **1997**, *56*, 1809–1819.
- [35] J. C. Swarbrick, Y. Kvashnin, K. Schulte, K. Seenivasan, C. Lamberti, P. Glatzel, *Inorg. Chem.* **2010**, *49*, 8323–8332.
- [36] E. Gallo, C. Lamberti, P. Glatzel, *Phys. Chem. Chem. Phys.* **2011**, *13*, 19409–19419.
- [37] K. Seenivasan, E. Gallo, A. Piovano, J. G. Vitillo, A. Sommazzi, S. Bordiga, C. Lamberti, P. Glatzel, E. Groppo, *Dalton Trans.* **2013**, *42*, 12706–12713.
- [38] A. A. da Silva, M. D. M. Alves, J. H. Z. dos Santos, *J. Appl. Polym. Sci.* **2008**, *109*, 1675–1683.
- [39] S. I. Troyanov, E. M. Snigireva, V. B. Rybakov, *Zhurnal Neorg. Khimii* **1991**, *36*, 1117–1123.
- [40] I. Pollini, *Solid State Commun.* **1983**, *47*, 403–408.
- [41] C. H. Maulet, J. N. Tothill, P. Strange, J. A. Wilson, *J. Phys. C: Solid State Phys.* **1988**, *21*, 2153–2179.
- [42] A. Leon, O. Kircher, J. Rothe, M. Fichtner, *J. Phys. Chem. B.* **2004**, *108*, 16372–16376.
- [43] U. Bergmann, C. R. Horne, T. J. Collins, J. M. Workman, S. P. Cramer, *Chem. Phys. Lett.* **1999**, *302*, 119–124.
- [44] S. A. Pizarro, P. Glatzel, H. Visser, J. H. Robblee, G. Christou, U. Bergmann, V. K. Yachandra, *Phys. Chem. Chem. Phys.* **2004**, *6*, 4864–4870.
- [45] E. Gallo, F. Bonino, J. C. Swarbrick, T. Petrenko, A. Piovano, S. Bordiga, D. Gianolio, E. Groppo, F. Neese, C. Lamberti, P. Glatzel, *ChemPhysChem* **2013**, *14*, 79–83.
- [46] L. Sementa, M. D'Amore, V. Barone, V. Busico, M. Causa, *Phys.Chem.Chem.Phys.* **2009**, *11*, 11264–11275.
- [47] ADF2013, *SCM, Theoretical Chemistry, Vrije Universiteit, Amsterdam, The Netherlands*, <http://www.scm.com>.
- [48] G. te Velde, F. M. Bickelhaupt, E. J. Baerends, C. Fonseca Guerra, S. J. A. van Gisbergen, J. G. Snijders, T. Ziegler, *J. Comput. Chem.* **2001**, *22*, 931–967.
- [49] J. P. Perdew, K. Burke, M. Ernzerhof, *Phys. Rev. Lett.* **1996**, *77*, 3865–3868.
- [50] S. Grimme, J. Antony, S. Ehrlich, H. Krieg, *J. Chem. Phys.* **2010**, *132*.
- [51] E. van Lenthe, E. J. Baerends, *J. Comput. Chem.* **2003**, *24*, 1142–1156.
- [52] E. van Lenthe, A. Ehlers, E. J. Baerends, *J. Chem. Phys.* **1999**, *110*, 8943–8953.

---